The Development of a CO_2 Test Capability in the NASA JSC Arc Jet for Mars Entry Simulation

Steven Del Papa[*]

NASA Johnson Space Center, Houston, TX, 77058

Leonard Suess, Ph.D.[†]

Jacobs Engineering, Houston, TX, 77058

Brian Shafer[‡]

Jacobs Engineering, Houston, TX, 77058

The Atmospheric Reentry Materials and Structures Evaluation Facility (ARMSEF) located at NASA Johnson Space Center is used for simulating the extreme environment experienced upon reentry for the development and certification of thermal protection systems (TPS). The facility supports a large variety of programs and was heavily leveraged for the certification and operational support of the TPS for the Orbiter and, more recently, the development of the heat shield for CEV.

Unique attributes of the facility include a modular aerodynamically stabilized arc heater and independently controlled O_2 and N_2 for the test gases. When combining the O_2 and N_2 in a 23:77 mass ratio respectively the Earth's atmosphere is accurately simulated and via modification of this ratio the investigation of the effects of atomic oxygen on a material's response is possible. In the summer of 2010 a development effort was started to add CO_2 as a third independently controlled test gas to open up the the possibility of accurately simulating a Martian reentry environment on larger test articles due to the 13MW power capability of the test facility.

Initial testing involved relatively low concentrations of CO_2 combined with N_2 for the primary purpose of gathering data to answer two pressing safety concerns. The first being the rate of production of carbon monoxide (CO) within the ejector vacuum system and how to safely manage the concentrations to prevent flammable or possibly explosive conditions. The second safety concern addressed is the possible formation of hydrogen cyanide (HCN) and cyanide (CN). HCN would primarily be present in the cooling water while the CN would most probably condense out and plate the interior surfaces of the test chamber. Water samples and wipes of the test chamber surfaces were analyzed for the presence of HCN and CN.

In addition, heat flux and pressure probe data as well as laser induced fluorescence (LIF) data of atomic oxygen for CO_2:N_2 and enriched O_2 flowfields will be presented.

I.   Introduction

ARCJET facilities have been in use since the 1950s to simulate spacecraft re-entry environments for the development and certification of thermal protection materials and systems.[1] Briefly, test articles, constructed to represent spacecraft structures, are immersed in a high enthalpy flow that provides a relevant heating rate, pressure, and chemically reactive environment experienced within the hypersonic regime. The ARMSEF, an arc jet facility used to simulate earth reentry conditions, located at NASA Johnson Space Center (JSC) was primarily used to develop, evaluate, and certify every type of TPS used on the Apollo Command Module and the Space Shuttle Orbiter vehicle.[2] The facility was also heavily relied upon for

---

[*]Aerospace Engineer, ES3/Thermal Design Branch

[†]Research Scientist, Jacobs Engineering, 2101 NASA Parkway

[‡]Chemical Engineer, Jacobs Engineering, 2101 NASA Parkway

operational support throughout the life of the Orbiter program for vendor requalifications, anomaly resolutions, design changes, and TPS upgrades that introduced new materials. TPS damage tolerance and TPS repair materials and techniques were characterized with a large amount of arc jet testing as a part of the return to flight (RTF) effort after the loss of Columbia in 2003. The implementation of the inspection of the TPS during Orbiter missions resulted in arc jet testing during the STS-117 and STS-118 missions after damage to the TPS was discovered. With the cessation of the Orbiter program in 2011 the ARMSEF has become available to support a wider variety of programs. Some of the programs supported are Commercial Crew Development (CCDev), Entry Descent Landing (EDL),[3] Adaptive Deployable Entry and Placement Technology (ADEPT),[4] and the Inflatable Re-entry Vehicle Experiment (IRVE-3).[5] A significant portion of test time has also been (and still is) devoted to the Crew Exploration Vehicle (CEV) heatshield development and characterization. All test programs performed in the ARMSEF to date have been for an Earth entry environment. With an increased awareness for spacecraft missions to Mars, there is a steadily increasing desire for providing a simulated entry environment that is predominately comprised of CO_2. Considering the fact that the response of most TPS materials being considered for a Mars mission is heavily dependent on the chemical composition of the flowfield, the ability to test in CO_2 will provide data for more accurate models that in turn result in a more optimized heatshield design.

A.   ARMSEF Facility

The arc heater is a dual-diameter constricted arc column consisting of a tungsten button cathode as the upstream electrode and a conical copper anode is used as the downstream electrode. The arc heater contains 200 individually water-cooled, electrically-isolated constrictor segments; assembled in modular packs, 20 segments per pack. Packs can be removed from or added to the heater to provide an expanded operational envelope. The 15 degree half-angle conical nozzle in TP2 is of a modular design allowing for exit diameters from 5 inches to 40 inches, in 5 inch increments.

Figure 1. Photograph of TP2

There are also special nozzle segments that create a 3.5 inch and a 7.5 inch diameter exit. Normally a 2.25 inch diameter throat is used but a 1.25 and a 1.90 inch diameter throats are available as well. A photograph of TP2 is presented in Figure 1. For an Earth environment the test gas is 23 percent O_2 and 77 percent N_2 by mass, which is injected at various places along the column's length. For a tungsten cathode button, N_2 is always injected in the vicinity of the cathode to prevent oxidation of the tungsten.

The test gas is injected tangential to the inner column diameter so that a vortex is formed. This vortex stabilizes the electric arc, which heats the gas mixture as it flows down the column length from cathode to anode. The electrically heated test gas then expands through the nozzle and enters into the test chamber at supersonics speeds. As the heated gasses pass over the surface of the test article, the required surface temperatures and pressures are generated. The test article front face can be situated at a variable distance from the nozzle exit plane which is referred to as the Z-distance.

II.   Mars Entry Environment

A.   Rationale for a CO_2 Arc Jet

The ARMSEF simulates the Earth's atmosphere with individually controlled O_2 and N_2 test gas systems that deliver a 23:77 O_2:N_2 mass ratio within the arc heater. One major advantage of this configuration is the ability to dynamically adjust the O_2 ratio through the control system, from 0% up to 65%. The Mars Science Lab (MSL) spacecraft is using a phenolic impregnated carbon ablator (PICA) as the heatshield, and in 2008 four PICA models were tested in the arc jet at varying O_2 ratios (see Figure 2) to better understand the impact of the atomic oxygen on the performance of this material.

All four PICA models were exposed to equivalent heating rates, impact pressures, and exposure durations, and a correlation of increased recession to increased oxygen content was evident. The increased recession of the PICA models due to increased oxygen content highlights one important reason for using a CO_2 rich arc jet. Since the atmosphere of Mars can contain as

Figure 2.   Effect of PICA behavior with O_2 Variation.

much as 97% CO_2 by volume, it is evident that a greater understanding of TPS response to this radically different environment is required for accurate modeling and robust design to ensure mission success. For low enthalpy conditions, atomic oxygen facilitated through the dissociation of CO_2 via the reaction,[6]

$$CO_2 \rightarrow CO + O - 2.9\,eV/molecule \tag{1}$$

could prove to be a significant source of atomic oxygen comprising more than 35% of the gas composition by mass. Furthermore, with increasing gas enthalpy the formation of $\sim$ 70% atomic oxygen (by mass) is possible through the dissociation of CO via the reaction,

$$CO \rightarrow C + O - 11.2\,eV/molecule. \tag{2}$$

With several planned missions to Mars such as the Scout Program's small mission Mars Atmosphere and Volatile Evolution (MAVEN) in 2013 and the combined NASA/ESA dual-rover mission planned for 2018, the need for ground-based testing of TPS materials within a Martian atmospheric entry condition is essential for current Mars entry simulations.[7] Current models[8,9] for a vehicle entry speed into Mars ranging from 5 - 10 km/s show no significant dissociation of CO; therefore, Equation 1 should be the dominating source of atomic oxygen within Mars atmosphere entry flows. Moreover, the recombination reactions of $CO + O \rightarrow CO_2$ and $O + O \rightarrow O_2$ with the TPS surface could prove to be an important factor to the total heat flux[10] with some models indicating that the heat flux due to catalycity in a simulated Martian atmosphere could be approximately two times more than in Earth's air.[11] The development of a ground-based CO_2 test facility can; therefore, provide crucial data for TPS modeling within a Mars-like plasma.

III.   Safety Mitigation

Achieving a self-sustaining Mars-like plasma required the implementation of a CO_2 and N_2 test gas system. Modifications to the normal configuration were performed to allow for the CO_2 test gas. The feed rate of CO_2 has been performed incrementally to help identify all safety concerns which primarily focused on the creation of carbon monoxide (CO), cyanide (CN) and hydrogen-cyanide (HCN) since these products are poisonous; furthermore, the formation of CO in the presence of O_2 creates a possible explosive environment. Additionally, Deposition of carbon on internal heater surfaces could easily lead to a catastrophic short circuit.

A.   Carbon Monoxide

The lower explosive limit (LEL) and upper explosive limit (UEL) for carbon monoxide-air mixtures is listed as 12 % and 75% respectively by volume for standard temperature pressure environments.[12] To mitigate
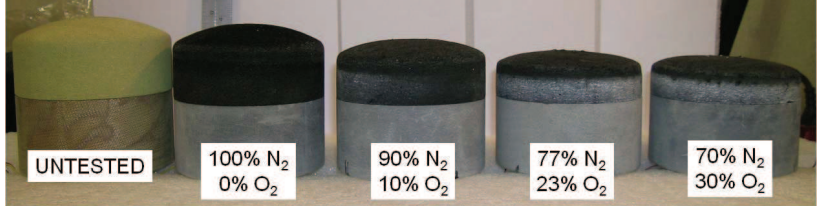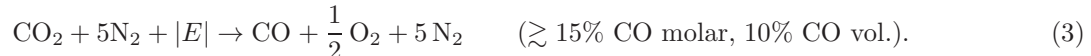
the explosive concern, the IRS plasma wind tunnel (PKW 3) use N_2 as a dilutant. Herdrich et. al[13] eluded that a dilution ratio of 5:1 $N_2 : CO_2$ is needed for safety mitigation. This dilution makes it stoichiometricly impossible to create an explosive environment even at 100% molar conversion of CO_2 to CO

$$CO_2 + 5N_2 + |E| \rightarrow CO + \frac{1}{2}O_2 + 5N_2 \qquad (\gtrsim 15\% \text{ CO molar, } 10\% \text{ CO vol.}). \tag{3}$$

Initially, 100% conversion of CO_2 to CO was assumed and a stoichiometric N_2 dilution of 5:1 into the heater and very small CO_2 flow rates were used.

To better define the needed dilution ratios, chemical modeling was performed by NASA / White Sands Test Facility (WSTF) and Sandia National Laboratories (SNL).[14] A worst case conversion rate of $\sim$52% CO_2 to CO was predicted. Using this conversion rate, allowed for adjustment (with margin) of the CO_2 flow rate and N_2 dilution. Consequently, the second CO_2 test indicated an empirical molar conversion rate of 60% CO_2 to CO.

B. Cyanide

Cyanide production is also possible in the CO_2 plasma process. The White Sands Test Facility and Sandia National Labs chemical modeling predicted a worst case cyanide formation at a rate of $\sim$0.146% via the reaction

$$CO_2 + N_2 + |E| \rightarrow CN^- + O_2 + \frac{1}{2}N_2. \tag{4}$$
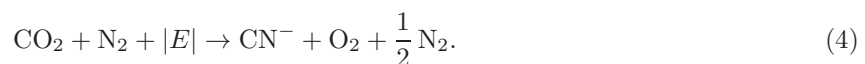
Further interaction of the cyanide ion with the steam from the steam ejector, can produce hydrogen cyanide via the reaction

$$CN^- + H_2O \rightarrow HCN + OH^-. \tag{5}$$

A Residual Gas Analyzer (see Section D) system has been used to allow for the detection of cyanide and hydrogen cyanide with no observations of it to date. After every test, the JSC Industrial Hygiene (IH) office collects samples from various locations within the arc column and test chamber. These samples are then analyzed for cyanide and hydrogen cyanide content. To date, all samples have been reported as "non-detect" ($< 1\,\mu g/ft^2$). Liquid samples of the cooling water and steam condensate were also analyzed for other cyanide compounds such as Nickel Carbonyl with all results non-detected as well. Continued use of both the RGA and IH analysis will be performed when new test conditions are attempted until the limits of the operating envelope have been achieved.

C. Carbon Deposition

The formation of carbon has been observed in other arc heaters using a CO_2 test gas such as the Hypersonic Materials Environmental Test System (HyMETS) - NASA/LaRC. Complete disassociation of the CO_2 can deposit carbon in the form of soot on the internal heater parts causing heater segments to short and could lead to a catastrophic short of the heater itself via the reaction

$$CO_2 + |E| \rightarrow C(s) + O_2. \tag{6}$$

Visual inspection of the heater and chamber has not indicated any carbon soot formation. Wipe samples for total organic composition have been analyzed by the IH office, but the levels are too low to connect to the CO_2 plasma as the source. The RGA has not detected any carbon (12 amu) levels. Visual inspection of the test chamber and arc column will continue throughout the development.

D. Residual Gas Analyzer

To monitor the chemical composition of the gas exiting the exhaust of the test chamber, a residual gas analyzer system was installed. A gas sampling port was drilled into the after-cooler of the TP-2 diffuser, a vacuum system (Pfieffer Vacuum HiPace-80 Pumping Station) - to transport the sampled gas stream, and a residual gas analyzer (Stanford Research Systems RGA300) to measure the spectrum of mass-to-charge ratios of the gas species. The sampling port is located downstream from the water-cooled after-cooler that cools the exhaust stream and causes a shock wave that converts the supersonic flow to subsonic. Immediately upstream

from the after-cooler, the temperature of the gas ($\sim 1500°F$) is likely to damage sensitive components within the RGA.

A metering valve allows for precise pressure control in the range of $\approx 10^{-8}$ Torr to 10^{-4} Torr where the upper pressure limit is defined by the working parameters for the RGA. The sampling tube is connected using standard vacuum fittings to valves and a 12-foot-long section of 1" ID flexible stainless-steel vacuum tubing that connects to the vacuum system. The long tube was necessary because of the distance between the vacuum pump system and the sampling point.

The RGA is a quadrupole mass spectrometer that is controlled using software written for this particular experiment. The RGA output indicates partial pressure for a range of species according to the ratio of mass to charge (M/Q) of the species. Consequently, there is ambiguity between, for example, singly-ionized nitrogen and carbon monoxide, both having M/Q = 28. A significant amount of interpretation of the data is required, and one must make use of auxiliary information. For example, when sampling air, signals at M/Q = 28 indicate molecular nitrogen, whereas when using a rich CO_2 gaseous atmosphere, both carbon monoxide and nitrogen will contribute to the M/Q = 28 signal. To circumvent any misinterpretation of the data, all tests involving CO_2 were conducted in pulsed mode. During one CO_2 test, the arc plasma is initially maintained with pure N_2 and CO_2 is injected into the arc-column for a pre-determined time (Δt. After time Δt has elapsed, the CO_2 source is switched off while the N_2 source continues to be injected into the arc column. The RGA system samples the exhaust gas throughout the entire test duration; therefore, plotting M/Q as a function of time (Figure 3) will yield the net contribution due carbon monoxide at 28 amu.
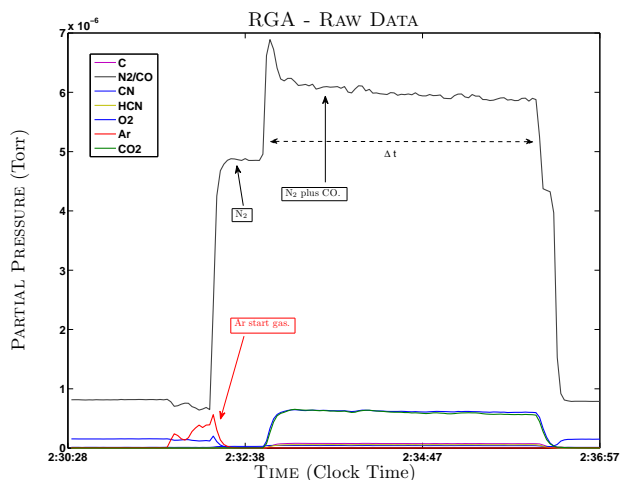
Figure 3. Sample RGA results for cool gas composition (90:10 CO_2 : N_2). M/Q as a function of time. The vertical arrows represent time intervals referring to only N_2 injection and $CO_2 + N_2$ respectively.

From the RGA system data, it is deduced that $\sim 60\%$ (molar) of CO_2 injected into the arc column is converted to CO immediately following the after-cooler. It is worth noting for the current tests (and all previous tests) that the conversion rate from CO_2 to CO remained almost constant independent of input current. Since the gas sampled for the RGA occurs when the gas is rapidly cooled, the M/Q profile does not necessarily reflect the plasma conditions within the testing chamber. The RGA data also point to no formation of CN, HCN, or carbon within the exhaust gas.

IV.   Flowfield Analysis - Laser Induced Fluorescence

Two-photon LIF (2P-LIF) spectroscopy and its application to gas-phase diagnostics for arc jet flow streams have been studied extensively and described previously.[15, 16, 17] Briefly, light from an ultraviolet tunable laser source electronically-excites ground state atomic oxygen $(2p^4\,{}^3P_J)$ through the simultaneous absorption of two photons into an upper state $(3p\,{}^3P_J)$. The excited atomic oxygen then fluoresces a near-infrared photon (845 nm) as the excited electron decays into an intermediate state $(3s\,{}^3S)$ as illustrated in Figure 4. This emitted fluorescence signal is recorded as the laser wavelength is scanned over the absorption feature. The magnitude of the spectrally integrated fluorescence profile is proportional to the number density of the absorbing state and the square of the incident laser pulse energy.

A schematic of the 2P-LIF application to an arc jet flow stream is shown in Figure 5. The excitation laser beam intersects the flow axis at a non-normal angle ($\theta \sim 23°$). Photons emitted by the atomic target during fluorescence are collected from a small volume defined by the intersection of the laser beam and the region subtended by the collection optics. The probe volume is aligned to point on the flow axis at eight inches from the nozzle exit. A red-sensitive photomultiplier tube (PMT) and gated socket (Hamamatsu R636-10, C1392) are used to collect the fluorescence signal. Spectral and neutral density filters positioned between the collection optics and PMT

Figure 4. Energy level schematic for atomic oxygen excitation.

ensure only light originating from atomic fluorescence is collected and analyzed. The measured excitation line-shape is analyzed to determine the Doppler shift in the absorption wavelength, Doppler width, and integrated signal intensity, from which the flow velocity, temperature, and absolute atomic density, respectively, can be extracted.[18]
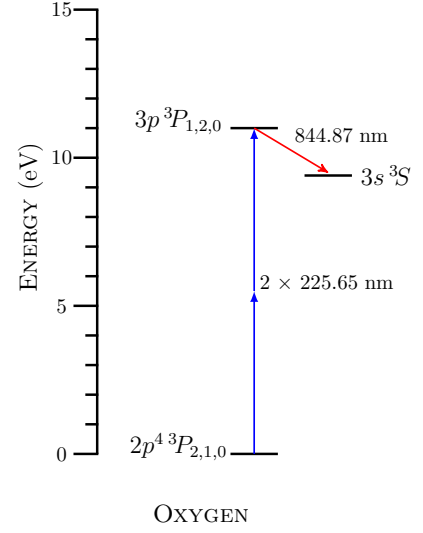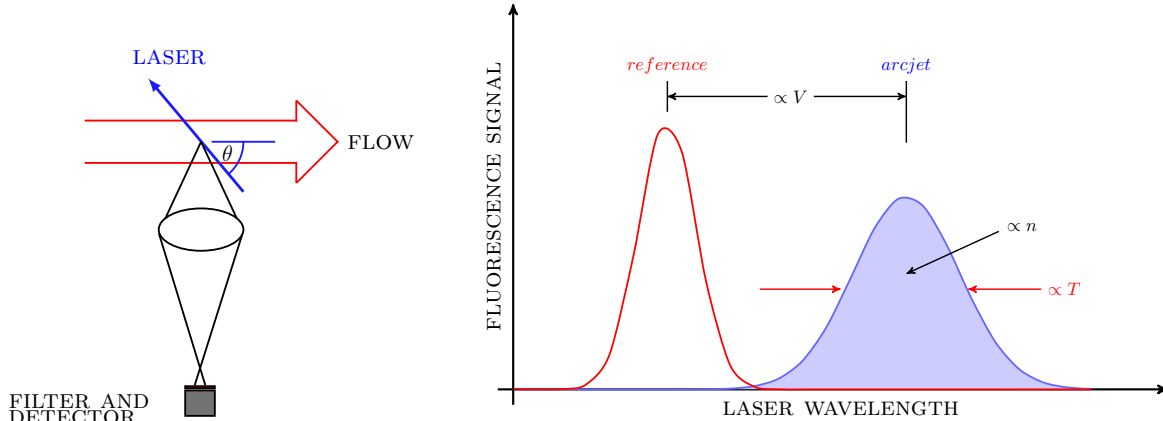
Figure 5. Schematic of the 2P-LIF application to an arc jet flow stream. Velocity of the atomic species is obtained from the frequency shift of the absorption feature. Temperature is extracted from the Doppler broadening of the excitation line-shape. The ground-state density of atoms is obtained from the integral of the excitation line-shape.

A.   Experimental Setup

A simplified scheme of the experimental set-up is depicted in Figure 6 . A tunable 30 Hz Nd:YAG (Continuum Powerlite Precision 9030) pumped dye laser (Continuum ND6000) provides visible radiation from 612 nm to 690 nm. The output of the dye laser is frequency-tripled using two auto-tracking crystal assemblies (Inrad AT-III) equipped with two beta-BaB$_2$O$_4$ ("BBO") crystals resulting in   8 ns pulses of vertically
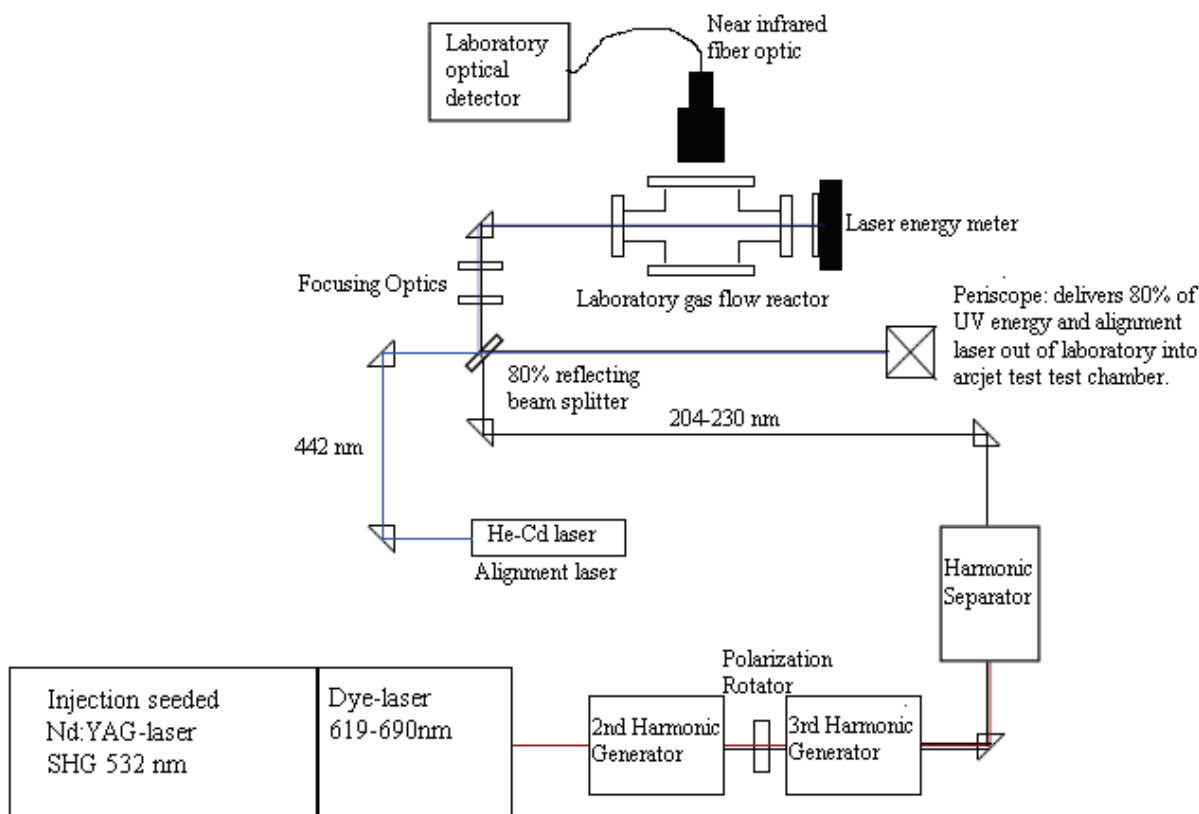
Figure 6. Schematic diagram of the laboratory laser and optical configuration.

polarized coherent ultraviolet light between 204 nm and 230 nm with a pulse energy up to 4 mJ and a spectral bandwidth of approximately 0.09cm^{-1}. A four-prism harmonic separator is employed to separate the third harmonic laser beam from the dye laser fundamental and second harmonic laser beams. The two BBO crystals are automatically angle tuned using active feedback circuitry to provide constant output energy while scanning the dye laser wavelength. To access the atomic oxygen transitions, LDS 698 (Exciton) is used. Approximately 20% of the UV laser beam pulse energy is reserved for frequency and calibration measurements in the laboratory flow reactor. A pyroelectric energy sensor monitors the pulse energy directed through the flow reactor. The remaining 80% is directed out of the laboratory to the arc jet test cabin using a Class I fully enclosed laser beam transmission path.

The optical configuration for these tests was designed to enable single point LIF measurements on the flow centerline at a prescribed location 8 inches downstream of the nozzle exit. The laser beam enters the test chamber (TP-2) through a dedicated fused-silica window. Mounted on the inside wall of TP-2 is an enclosed optical assembly that focuses the laser beam after it passes through the window. An aluminum mirror directs the laser beam upstream to intersect the nozzle axis at a prescribed distance downstream of the nozzle exit. As the overlap of the focused beam path with the region imaged by the collection optics is critical for repeatable absolute 2P-LIF intensity measurements, remotely controlled actuators operated from the laboratory are used to correct misalignment caused by cabin wall deflections or thermal drifts of the optics.

The excited fluorescence is imaged from the probe volume and directed outside the test chamber through a 1.37-inch clear aperture window located on the front face of TP-2. The primary objective optic is a 3 inch diameter lens (Newport KPX232.AR16) situated 11.75 inches from the center-line of the flow. A four inch protected gold surface mirror directs the imaged fluorescence horizontally to the integrated optical receiver which is located directly outside the vacuum chamber (TP-2).

B. Calibration

In order to determine the flow velocity, temperature, and absolute atomic density, a stable reference source of atomic oxygen of a known concentration is needed. A low-pressure ($10^{-4} - 10$ Torr) laboratory flow apparatus constructed from quartz tubing and fittings was designed to produce atomic oxygen under controlled conditions. Gas flow rates into the flow reactor are monitored by mass flow controllers, and a pressure controller and downstream throttle valve maintain a prescribed pressure in the flow reactor. Generating atomic oxygen (from an O_2 source) is accomplished by electron impact dissociation in a microwave discharge (2.45 GHz, 60 W) which drives a cylindrical resonator surrounding a quartz tube inlet arm of the flow reactor. A separate quartz inlet "mixing ball" located 8 cm upstream of the detection volume allows for the use of additional gases into the main flux in a controlled manner. The flow reactor has optical access windows for the probe beam and fluorescence collection.

Determining the absolute atomic oxygen density within the flow reactor is accomplished via titration according to the following fast reaction:[19]

$$O + NO_2 \rightarrow NO + O_2. \tag{7}$$

Determination of the absolute atomic oxygen density is performed using a similar procedure detailed by Niemi et al.[20] Briefly, titration gas (1.996% NO_2 gas balanced with He) is added through the mixing ball into the main flux, and the on-resonance 2P-LIF oxygen signal is measured as a function of titration gas flux. As the titration gas flux is increased, the atomic oxygen 2P-LIF signal decreases linearly until the signal extinguishes. Assuming complete reaction of titrant gas with oxygen, each NO_2 molecule leads to the consumption of one oxygen atom. When the 2P-LIF signal approaches zero, the NO_2 flux (φ_{NO_2}) equals the initial oxygen atom flux (φ_O); therefore, at the titration point the O concentration is the same as the NO_2 concentration in the absence of O. The 2P-LIF calibration measurements are made at the titration point. The procedure for obtaining absolute atomic oxygen density measurements in the arc jet relies upon 2P-LIF measurements of Xe, respectively, using the same experimental configurations. The flow reactor was also designed to accommodate controlled gas flows of Xe buffered with helium at prescribed flow rates and pressures, creating known concentrations of Xe for transfer-standard 2P-LIF measurements in the laboratory.

Calibration using 2P-LIF of Xe in the arc jet facility is accomplished with a small quartz flow cell placed at the measurement location. The cell has optical access for the probe beam and fluorescence collection. It is supplied with a metered mixture of Xe/He at a prescribed pressure using identical mass flow and pressure control components as the laboratory flow reactor. A mobile flow system contains the gas control components, gas supplies, vacuum pump, and computer for flow system operation. Attached to the gas cell is a pyroelectric energy sensor for pulse energy measurement at the cell exit window. The gas cell is aligned with the intersection of the probe laser and receiver optical paths at the measurement location.

V. Conclusions

A. 2P-LIF Results

Dedicated arc jet tests were made available for the present investigation to better understand the flow-field behavior using a CO_2 rich injection scheme. Test conditions were selected such that one parameter, the oxygen content by mass, was varied within the arc column to compare with the hypothetical case of complete dissociation of CO_2. Since it has been shown that the percent of O_2 within the arc column greatly influences the recession rate of PICA, trying to characterize the atomic oxygen differences between a CO_2 rich and an O_2 rich injection scheme for moderate to high arc power was our initial goal. Results of using 2P-LIF to probe the different plasmas created through the different injection methods will now be discussed. The results for all dedicated arc jet tests are presented in Table 1.

Spectra from 2P-LIF measurements of atomic oxygen are presented in Figure 7 with the corresponding $CO_2 : N_2$ mixture. Run # 3710 yields oxygen 2P-LIF results for similar total mass flow and power levels, but heat flux and pressure (as measured by a 4-in. diameter flat face calorimeter) were not fixed. The gas mixtures were chosen with the assumption of complete dissociation of $\sim$46% CO_2; therefore, the amount of O_2 present by mass would be $\sim$33%. The 2P-LIF results for run # 3710 with an arc current of 500 Amps are shown in Figure 7(a) and Figure 7(b) for the 46:64 $CO_2 : N_2$ and 33:67 $O_2 : N_2$ cases respectively. Increasing the arc current to 1000 Amps yielded only slight increases in atomic oxygen density, speed and temperature.
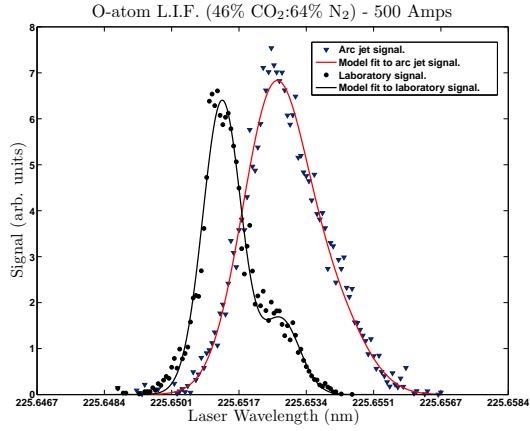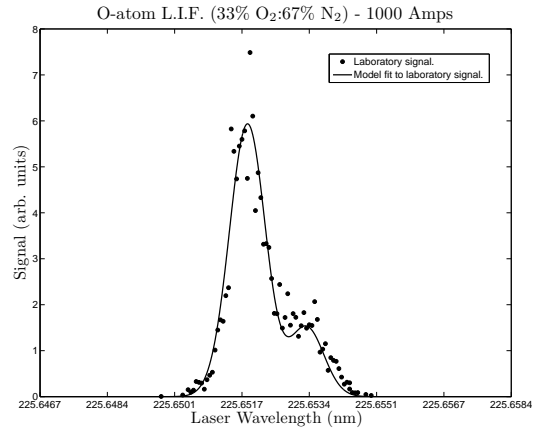
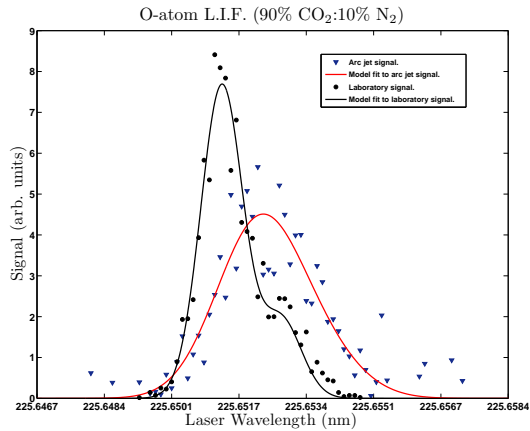(a) Oxygen atom 2P-LIF spectrum. Source: $46\%CO_2$:$64\%N_2$ at 500 Amps.
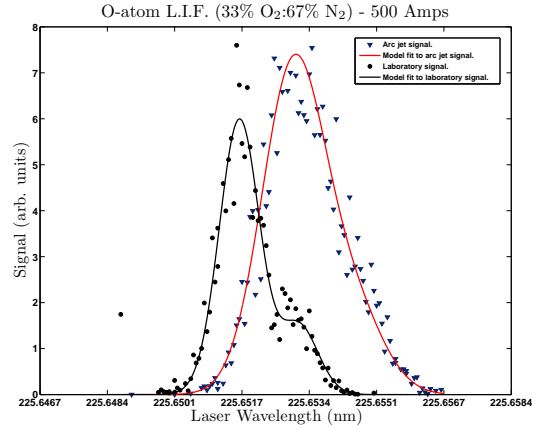
(b) Oxygen atom 2P-LIF spectrum. Source: $33\%O_2$:$67\%N_2$ at 500 Amps.
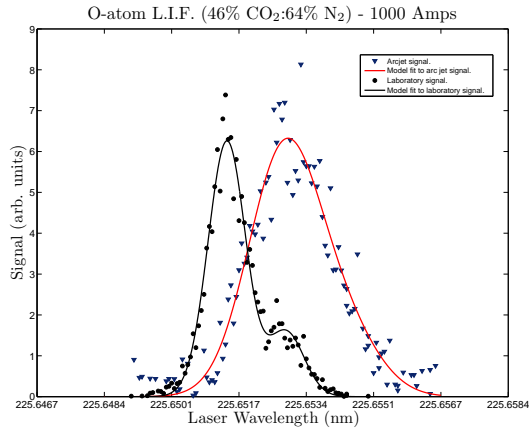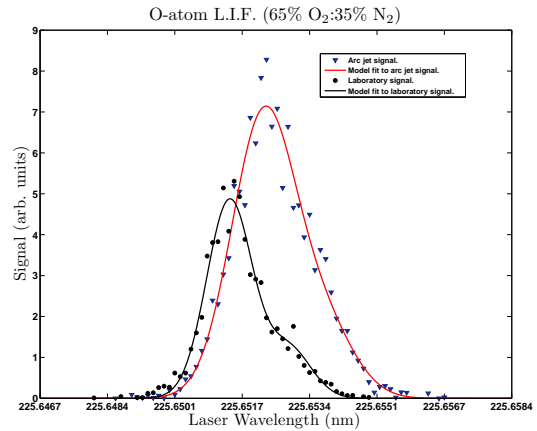
(c) Oxygen atom 2P-LIF spectrum. Source: $33\%O_2$:$67\%N_2$ at 1000 Amps.

(d) Oxygen atom 2P-LIF Laboratory spectrum. Background signal at 1000 Amps too dominating for data analysis.

(e) Oxygen atom 2P-LIF spectrum. Source: $90\%CO_2$:$10\%N_2$.

(f) Oxygen atom 2P-LIF spectrum. Source: $65\%O_2$:$35\%N_2$.

Figure 7. Comparison of oxygen atom 2P-LIF spectrums from different sources.

Unfortunately, significant amounts of background light passing through the spectral filter (830 - 850 nm) prohibited data analysis for the 33:67 O_2 : N_2 case.

Run #-3730 with CO_2 shown in Figure 7(e) has a smaller spectrally integrated signal than the enriched oxygen case (Run #-3728) shown in Figure 7(f). Under the assumption that the CO_2 molecule is completely dissociated for Run #-3730, the amount of O content by mass is $\sim 65\%$. Two 2P-LIF scans were performed for Run#-3730 due to a constant, low-level emission of background light passing through the 835 - 845 nm filter. The source of the background light was due to the plasma flow-field conditions. No such emission was noticed for Run #-3728.

Data from both runs (3728 and 3730), indicate that at the current enthalpy conditions CO molecules do not significantly dissociate within the arc column. This is reflected in the number density estimation from 2P-LIF where the density of atomic oxygen from dissociated O_2 is roughly double that of atomic oxygen generated by the CO_2 plasma. 2P-LIF data point to a possible scenario - for current enthalpy levels - where the CO within the arc column remains molecular. This is not totally unexpected since CO has a larger dissociation energy than N_2. The work performed by Cosby[21] indicates that the atomic fragments resulting from CO dissociation should be extremely "hot"; therefore, it is expected that the 2P-LIF spectral profile will change upon dissociation of CO to reflect hotter atomic species (spectrally broader) and possibly with an increase in speed (larger separation between reference and arc jet peaks). With no significant electrode erosion or carbon deposits within the arc column (as noted at the NASA/LaRC - HyMETS facility), it is speculated that the CO within the arc column is acting as a shield gas; therefore, prohibiting rapid oxidation of the electrodes.

While keeping heat flux and pressure constant, the thermal broadening of the spectral curve from 2P-LIF indicates that the atomic oxygen liberated from CO_2 is systematically hotter (almost double) than those liberated from the enriched O_2 case. No noticeable difference in the speeds of the atomic oxygen from both the CO_2 and O_2 schemes were noticed.

VI.   Forward Work

The JSC CO_2 arc jet is still in its infancy with a total of 10 tests with CO_2 as the test gas. JSC plans to develop the broadest CO_2 operational envelope and capabilities possible in the coming years and in parallel interrogate the flow field to gain complete understanding of its chemistry and how it relates to different test gases. In order to do this, many equipment upgrades and new operational schemes will need to be developed for safe and efficient operation of the heater.

A.   Martian Entry Conditions

The highest CO_2 test gas ratio in the JSC arc jet thus far has been 90%. JSC has developed a new operational scheme that will allow testing with 97% CO_2 3% N2 by volume in the near future. The new scheme will change the way the heater is started and the delivery of the test/dilution gas. This new scheme should decrease electrode erosion and improve the stability of the flow field.

B.   Power/Flow Rate Limits

One goal of the JSC arc jet is to push the operational envelope to 13 MW and 0.6 lbm CO_2/sec. Most of the equipment to reach the goal is already in use. The facility is now capable of 13 MW however, a new cryogenic CO_2 test gas system will need to be installed. The design and equipment specifications for the gas system have been determined and JSC expects to install the system in FY12.

C.   Relationships

During the incremental steps toward 13 MW , 0.6 lb CO_2/sec JSC will be analyzing the flow field to determine the nature of CO_2/CO disassociation. From this investigation a disassociation map of all species involved should be determined. The disassociation data will also lead to comparisons of CO_2 to other test gas environments. The free oxygen content of CO_2 tests will be reproduced in O_2 rich tests. Ablator models will be used in both environments to determine the effects of C/CO in model regression.

D. Dust

To more accurately recreate Martian entry conditions, the frequent dust storms occurring on Mars must be included. JSC will be adding the capability to inject particles into the plasma flow to simulate the dust erosion and shock heating augmentation. A planned scheme uses CO_2 as a carrier gas for either SiC or alumina particles that are injected upstream of the nozzle throat. Optical methods can be used to determine the particle velocity profiles and spatial distribution

8th International Planetary Probe Workshop, June 6-10, 2011, Portsmouth, VA.

12 of 13

Run#	Facility Settings				2P-LIF Results			Facility Data				Comments
	N_2 Mass Flow (lbm/s)	CO_2 Mass Flow (lbm/s)	O_2 Mass Flow (lbm/s)	Current (Amps)	Temperature (°F) [K]	Speed (m/s)	Density $\times 10^{21}$ (m^3)	Power (MW)	Bulk Enthalpy (BTU/lb) [MJ/kg]	Pressure* (psf) [kPa]	Heat Flux* (BTU/(ft^{2}s) [MW/m^2]	
3710	0.119	0.104	–	500	2600 [1700]	4000	9.5	1.32	4170 [9.70]	155 [7.42]	148 [1.68]	**46% CO_2** **(by mass)**
3710	0.118	0.101	–	1000	3420 [2150]	4400	10.5	2.33	6670 [15.52]	200 [9.57]	352 [4.00]	**46% CO_2** **(by mass)**
3710	0.158	–	0.079	500	2400 [1590]	4120	10.4	1.37	3850 [8.96]	186 [8.90]	246 [2.79]	**33% O_2** **(by mass)**
3730	0.042	0.358	–	750	3900 [2400]	2510	2.9	2.56	4910 [11.42]	265 [12.69]	185 [2.10]	**90% CO_2** **(by mass)**
3730	0.042	0.358	–	750	4500 [2800]	2700	2.9	2.56	4910 [11.42]	265 [12.69]	185 [2.10]	**90% CO_2** **(by mass)**
3728	0.140	–	0.256	410	2100 [1400]	2575	5.7	1.33	2530 [5.89]	265 [12.69]	185 [2.10]	**65% O_2** **(by mass)**

Table 1. 2P-LIF Results for various test conditions.* Data acquired with a 4-in diameter flat face calorimeter.

References

[1]Scott, C. D., "Survey of Measurements of Flow Properties in Arcjets," *Journal of Thermophysics and Heat Transfer*, Vol. 7, No. 1, 1993, pp. 9–24.

[2]Rochelle, W. C., Battley, H. H., Grimaud, J. E., Tillian, D. J., Murray, L. P., Lueke, W. J., and Heaton, T. M., "Orbiter TPS Development and Certification Testing At the NASA/JSC 10 MW Atmospheric Reentry Materials and Structures Evaluation Facility," AIAA paper 83–0147, Jan. 1983.

[3]Beck, R. A. S., Arnold, J. O., White, S., Fan, W., Stackpoole, M., Agrawal, P., and Coughlin, S., "Overview of Initial Development of Flexible Ablators for Hypersonic Inflatable Aerodynamic Decelerators," AIAA paper 2011–2511, May 2011.

[4]Venkatapathy, E., Arnold, J., Fernandez, I., Hamm Jr., K. R., Kinney, D., Laub, B., Makino, A., McGuire, M. K., Peterson, K., Prabhu, D., Empey, D., Dupzyk, I., Huynh, L., Hajela, P., Gage, P., Howard, A., and Andrews, D., "Adaptive Deployable Entry and Placement Technology (ADEPT): A Feasibility Study for Human Missions to Mars," AIAA paper 2011–2608, May 2011.

[5]Jurewicz, D., Brown, G., Gilles, B., Lichodziejewski, L., Kelly, C., Tutt, B., and Hughes, S., "Design and Development of Inflatable Aeroshell Structure for IRVE-3," AIAA paper 2011–2522, May 2011.

[6]Eletskii, A. V. and Smirnov, B. M., "Dissociation of molecules in plasma and gas: the energy," *Pure and Applied Chemistry*, Vol. 57, No. 9, 1985, pp. 1235–1244.

[7]Wright, M. J., Tang, C. Y., Edquist, K. T., Hollis, B. R., Krasa, P., and Campbell, C. A., "A Review of Aerothermal Modeling for Mars Entry Missions," AIAA paper 2010–0443, Jan. 2010.

[8]Park, C., Howe, J. T., Jaffe, R. L., and Candler, G. V., "Review of Chemical-Kinetic Problems of Future NASA Missions, II: Mars Entries," *Journal of Thermophysics and Heat Transfer*, Vol. 8, 1994, pp. 9–33.

[9]Gallis, M. A. and Harvey, J. K., "Analysis of Non-Equilibrium in Mars Atmosphere Entry Flows," AIAA paper 95–2095, June 1995.

[10]Kolesnikov, A., Yakushin, M., Pershin, I., and Vasil'evskii, S., "Heat Transfer Simulation and Surface Catalycity Prediction at the Martian Atmosphere Entry Conditions," AIAA paper 99–4892, Jan. 1999.

[11]Paterna, D., Monti, R., Savino, R., and Esposito, A., "Experimental and Numerical Investigation of Martian Atmosphere Entry," *Journal of Spacecraft and Rockets*, Vol. 39, No. 2, 2002, pp. 227–236.

[12]Davletshina, T. A. and Nicholas P. Cheremisinoff Ph.D, *Fire and Explosion Hazards Handbook of Industrial Chemicals*, Noyes Publications, 1998.

[13]Herdrich, G., Löhle, S., Auweter-Kurtz, M., Endlich, P., Fertig, M., Pidan, S., and Schreiber, E., "IRS Ground-Testing Facilities: Thermal Protection System Development, Code Validation and Flight Experiment Development," AIAA paper 2004–22596, June 2004.

[14]White Sands Test Facility, "Carbon Monoxide Conversion Rates for NASA/JSC," Wstf–tr–11–01, WSTF, Las Cruces, NM, June 2011.

[15]Grinstead, J. H., Driver, D. M., and Raiche, G. A., "Radial profiles of arcjet flow properties measured with laser-induced fluorescence of atomic nitrogen," AIAA paper 2003–0400, Jan. 2003.

[16]Bamford, D. J., O'Keefe, A., Babikian, D. S., Stewart, D. A., and Strawa, A. W., "Characterization of arc-jet flow using laser-induced fluorescence," *Journal of Thermophysics and Heat Transfer*, Vol. 9, 1995, pp. 26–33.

[17]Flecher, D. J. and Bamford, D. J., "Arcjet flow properties determined from laser-induced fluorescence of atomic species," AIAA paper 98–2458, 1998.

[18]Fletcher, D., "Arcjet Flow Properties Determined from Laser-Induced Fluorescence of Atomic Nitrogen," AIAA paper 98–0205, 1998.

[19]Clyne M. A. A. and Nip W. S., *Reactive Intermediates in the Gas Phase ed D. W. Setser*, Academic Press, 1979.

[20]Niemi, K., Schulz-von der Gathen, V., and Döbele, H. F., "Absolute atomic oxygen density measurements by two-photon asborptoin laser-induced fluorescence spectroscopy in an RF-excited atmospheric pressure plasma jet," *Plasma Sources Science and Technology*, Vol. 14, 2005.

[21]Cosby, P. C., "Electron-impact dissociation of carbon monoxide," *Journal of Chemical Physics*, Vol. 98, No. 10, 1993, pp. 7804–7818.